

This is the accepted manuscript made available via CHORUS, the article has been published as:

# High-resolution study of Gamow-Teller transitions in the $^{47}\text{Ti}({}^3\text{He},t){}^{47}\text{V}$ reaction

E. Ganioglu *et al.*

Phys. Rev. C **87**, 014321 — Published 16 January 2013

DOI: [10.1103/PhysRevC.87.014321](https://doi.org/10.1103/PhysRevC.87.014321)

# High resolution study of Gamow-Teller transitions in the $^{47}\text{Ti}(^3\text{He}, t)^{47}\text{V}$ reaction

E. Ganioglu,<sup>1,\*</sup> H. Fujita,<sup>2,3,†</sup> Y. Fujita,<sup>2,3,‡</sup> T. Adachi,<sup>3</sup> A. Algara,<sup>4,5</sup> M. Csatlós,<sup>5</sup> J.M. Deaven,<sup>6,7,8</sup>  
 E. Estevez-Aguado,<sup>4</sup> C.J. Guess,<sup>6,7,8,§</sup> J. Gulyás,<sup>5</sup> K. Hatanaka,<sup>3</sup> K. Hirota,<sup>3</sup> M. Honma,<sup>9</sup>  
 D. Ishikawa,<sup>3</sup> A. Krasznahorkay,<sup>5</sup> H. Matsubara,<sup>3,¶</sup> R. Meharchand,<sup>6,7,8,\*\*</sup> F. Molina,<sup>4,††</sup>  
 H. Okamura,<sup>3,‡‡</sup> H.J. Ong,<sup>3</sup> T. Otsuka,<sup>10</sup> G. Perdikakis,<sup>6,7,8</sup> B. Rubio,<sup>4</sup> C. Scholl,<sup>11,§§</sup> Y. Shimbara,<sup>12</sup>  
 G. Susoy,<sup>1</sup> T. Suzuki,<sup>3</sup> A. Tamii,<sup>3</sup> J.H. Thies,<sup>13</sup> R.G.T. Zegers,<sup>6,7,8</sup> and J. Zenihiro<sup>3,¶</sup>

<sup>1</sup>*Department of Physics, Istanbul University, Istanbul 34134, Turkey*

<sup>2</sup>*Department of Physics, Osaka University, Toyonaka, Osaka 560-0043, Japan*

<sup>3</sup>*Research Center for Nuclear Physics, Osaka University, Ibaraki, Osaka 567-0047, Japan*

<sup>4</sup>*Instituto de Física Corpuscular, CSIC-Universidad de Valencia, E-46071 Valencia, Spain*

<sup>5</sup>*Institute of Nuclear Research of the Hungarian Academy of Sciences (ATOMKI), P.O.Box 51, H-4001 Debrecen, Hungary*

<sup>6</sup>*National Superconducting Cyclotron Laboratory, Michigan State University, East Lansing, Michigan 48824-1321, USA*

<sup>7</sup>*Joint Institute for Nuclear Astrophysics, Michigan State University, East Lansing, Michigan 48824, USA*

<sup>8</sup>*Department of Physics and Astronomy, Michigan State University, East Lansing, Michigan 48824, USA*

<sup>9</sup>*Center for Mathematical Science, University of Aizu, Aizu-Wakamatsu, Fukushima 965-8580, Japan*

<sup>10</sup>*Department of Physics, University of Tokyo, Hongo, Bunkyo, Tokyo 113-0033, Japan*

<sup>11</sup>*Institut für Kernphysik, Universität zu Köln, 50937 Köln, Germany*

<sup>12</sup>*Graduate School of Science & Technology, Niigata University, Nishi, Niigata, 950-2181, Japan*

<sup>13</sup>*Institut für Kernphysik, Westfälische Wilhelms-Universität, D-48149 Münster, Germany*

(Dated: January 2, 2013)

Given the importance of Gamow-Teller (GT) transitions in nuclear structure and astrophysical nuclear processes, we have studied  $T_z = +3/2 \rightarrow +1/2$ , GT transitions starting from the  $^{47}\text{Ti}$  nucleus in the  $(^3\text{He}, t)$  charge-exchange reaction at  $0^\circ$  and at an intermediate incident energy of 140 MeV/nucleon. The experiments were carried out at the Research Center for Nuclear Physics (RCNP), Osaka using the high resolution facility consisting of a high-dispersion beam line and the Grand-Raiden spectrometer. With an energy resolution of 20 keV, individual GT transitions were observed and GT strength was derived for each state populated up to an excitation energy ( $E_x$ ) of 12.5 MeV. The GT strength was widely distributed from low excitation energy up to 12.5 MeV, where we had to stop the analysis due to the high level density. The distribution of the GT strengths was compared with the results of shell model calculations using the GXPFI1 interaction. The calculations could reproduce the experimental GT distributions well. The GT transitions from the ground state of  $^{47}\text{Ti}$  and the  $M1$  transitions from the isobaric analog state in  $^{47}\text{V}$  to the same low-lying states in  $^{47}\text{V}$  are analogous. It was found that the ratios of GT transition strengths to the ground state, the 0.088 MeV, and the 0.146 MeV states are similar to the ratios of the strengths of the analogous  $M1$  transitions from the IAS to these states. The measured distribution of the GT strengths was also compared with those starting from the  $T_z = +3/2$  nucleus  $^{41}\text{K}$  to the  $T_z = +1/2$  nucleus  $^{41}\text{Ca}$ .

PACS numbers: 21.10.Hw; 21.60.Cs; 25.55.Kr; 27.40.+z;

## I. INTRODUCTION

Nuclear weak processes are crucial for the understanding of both nuclear structure and astrophysical processes. The most important nuclear weak processes are the Gamow-Teller (GT) transitions. In the  $pf$ -shell region, GT transitions starting from proton rich nuclei play important roles in the  $rp$ -process nucleosynthesis [1]. Therefore the study of GT transitions including those starting from unstable nuclei are of importance.

Studies of  $\beta$  decay can access the GT transitions from unstable nuclei. In addition, they give the most direct information on the GT transition strength  $B(\text{GT})$ . However, the excitation energies ( $E_x$ ) in the daughter nucleus accessible in  $\beta$  decay are limited by the decay  $Q$  values. In addition there is also a rapid decrease in feeding as  $E_x$  increases due to the decrease in the phase space factor. In contrast in charge-exchange (CE) reactions, such

---

\*Emailaddress:ganioglu@istanbul.edu.tr

†Emailaddress:hufujita@rcnp.osaka-u.ac.jp

‡Emailaddress:fujita@rcnp.osaka-u.ac.jp

§Present address: Department of Physics and Applied Physics, University of Massachusetts Lowell, Lowell, Massachusetts 01854, USA

¶Present address: RIKEN Nishina Center, Wako, Saitama 351-0198, Japan

\*\*Present address: Los Alamos National Laboratory, LANSCE-NS, Neutron & Nuclear Science, P.O. Box 1663, MS-H855, Los Alamos, New Mexico 87545, USA

††Present address: Comisión Chilena de Energía Nuclear, P.O. Box 188-D, Santiago, Chile

‡‡deceased

§§Present address: Institute for Work Design of North Rhine-Westphalia, Radiation Protection Services, 40225 Dusseldorf, Germany

as the  $(p, n)$ ,  $(n, p)$ ,  $(d, {}^2\text{He})$ ,  $({}^3\text{He}, t)$ , and  $(t, {}^3\text{He})$  reactions, one can observe GT transitions to states at higher energies without the  $Q$ -value limitation (e.g., see Refs. [2–6]). In CE reactions, at intermediate incident energies above 100 MeV/nucleon and forward angles around  $0^\circ$ , there is a close proportionality for GT excitations between the GT cross-sections and the  $B(\text{GT})$  values [7, 8]. Under these conditions,

$$\frac{d\sigma_{\text{GT}}}{d\Omega}(q, \omega) \simeq K(\omega) N_{\sigma\tau} |J_{\sigma\tau}(q)|^2 B(\text{GT}) \quad (1)$$

$$= \hat{\sigma}_{\text{GT}} F(q, \omega) B(\text{GT}), \quad (2)$$

where  $J_{\sigma\tau}(q)$  is the volume integral of the effective interaction  $V_{\sigma\tau}$ ,  $K(\omega)$  is the kinematic factor,  $\omega$  is the total energy transfer, and  $N_{\sigma\tau}$  is a distortion factor. The value  $\hat{\sigma}_{\text{GT}}$  is the “GT unit cross section” for a specific nuclear mass  $A$  at a given incoming energy and the value  $F(q, \omega)$  gives the dependence of the GT cross-sections on the momentum and energy transfers. It has a value of unity at  $q = \omega = 0$  and usually decreases gradually as a function of  $E_x$  and can be reliably obtained from DWBA calculations.

In the 1980s, pioneering  $(p, n)$  experiments at intermediate incident energies became possible and  $B(\text{GT})$  strength distributions were studied for various nuclei [3]. In particular, resonance structures in GT strengths [GT resonances, (GTR)] were systematically observed at  $E_x \approx 10$  MeV, which can not be observed in  $\beta$ -decay studies. In addition, in a recent pioneering  $(p, n)$  reaction using inverse kinematics, GT transitions from the  $T_z = 0$  unstable nucleus  ${}^{56}\text{Ni}$  have been studied [9].

The energy resolutions achieved in the  $(p, n)$  reaction studies were around 300 keV or greater. With these resolutions, it was difficult to resolve individual peaks lying close to each other in the excitation energy spectra.

The constraints imposed by the energy resolution were overcome by the use of the alternative  $({}^3\text{He}, t)$  reaction [5]. By applying precise beam matching techniques [10] to a magnetic spectrometer system, an energy resolution of 30 keV or less is possible at 140 MeV/nucleon and  $0^\circ$  in measurements with stable target nuclei. As a result, discrete states were observed not only in the low-lying region, but also in the GTR region of  $E_x \approx 10$  MeV [11].

The close proportionality given in Eq. (2) was examined by comparing the cross sections in  $({}^3\text{He}, t)$  measurements with the equivalent  $B(\text{GT})$  values from  $\beta$  decays for mirror GT transitions in  $sd$ -shell nuclei. Although some exceptional cases were recognized, the proportionality was generally good ( $\approx 5\%$ ) for “ $\Delta L = 0$ ” transitions in studies of the  $A = 23, 26, 27$ , and 34 nuclear systems [5, 12–15].

On the basis of these observations, the strengths of GT transitions starting from the  $T_z = +1$ ,  $pf$ -shell nuclei  ${}^{46}\text{Ti}$ ,  ${}^{50}\text{Cr}$ ,  ${}^{54}\text{Fe}$ , and  ${}^{58}\text{Ni}$ , and also the  $T_z = +4$  nucleus  ${}^{64}\text{Ni}$  have been intensively studied [11, 16–19]. The bump-like GTR structures consisting of many fragmented states were observed for nuclei  $A \geq 54$  but not

for the nuclei  $A \leq 50$ . As an extension of these studies, in this paper, we report the study of the GT transitions starting from the  $T_z = +3/2$  target nucleus  ${}^{47}\text{Ti}$  to the  $T_z = +1/2$  nucleus  ${}^{47}\text{V}$ . It should be noted that mirror GT transitions starting from the unstable nucleus  ${}^{47}\text{Mn}$  with  $T_z = -3/2$  to  ${}^{47}\text{Cr}$  with  $T_z = -1/2$  can be deduced from this study on the assumption that isospin symmetry holds in mirror transitions.

## II. EXPERIMENT

The states populated by GT transitions become prominent at intermediate energies and at forward angles near  $0^\circ$ . We performed the  ${}^{47}\text{Ti}({}^3\text{He}, t){}^{47}\text{V}$  measurement at the high energy resolution facility of the Research Center for Nuclear Physics (RCNP), Osaka using a high quality 140 MeV/nucleon  ${}^3\text{He}$  beam from the  $K = 400$  Ring Cyclotron [20]. This facility consists of a high-dispersion beam line “WS course” [21] and the Grand Raiden spectrometer [22] placed at  $0^\circ$ . The  ${}^3\text{He}$  beam was stopped by a Faraday cup placed inside the first dipole magnet.

A thin self-supporting  ${}^{47}\text{Ti}$  target with an isotopic enrichment of 94% and an areal density of 0.50 mg/cm<sup>2</sup> was used. The outgoing tritons were momentum analyzed within the full acceptance of the spectrometer and detected at the focal plane with a system consisting of two multi-wire drift-chambers (MWDC) that allow track reconstruction [23] and two plastic scintillators used for the creation of triggers to start the data acquisition system and particle identification.

An energy resolution of 20 keV [full width at half maximum (FWHM)] was realized by applying matching techniques [10] and the “faint beam method” [24, 25]. This resolution allowed us to resolve states in  ${}^{47}\text{V}$  up to  $E_x = 12.5$  MeV. The “ $0^\circ$  spectrum” for the  ${}^{47}\text{Ti}$  target with scattering angles  $\Theta \leq 0.5^\circ$  is shown in Fig. 1, where  $\Theta$  is defined by  $\sqrt{\theta^2 + \phi^2}$ . In order to obtain this spectrum, data were recorded for about half a day with a beam current of  $\approx 25$  enA on average. One can see the fine structure of fragmented states in Figs. 2 - 4.

In order to determine accurately the scattering angle  $\Theta$  near  $0^\circ$ , the scattering angles in both the  $x$  direction ( $\theta$ ) and  $y$  direction ( $\phi$ ) should be measured equally well. Good  $\theta$  resolution was achieved by using the *angular dispersion matching* technique [10], while good  $\phi$  resolution was achieved by applying the “over-focus mode” of the Grand-Raiden Spectrometer [26]. A more detailed description of the experimental procedure can be found in Ref. [18].

## III. DATA ANALYSIS

In  ${}^{47}\text{V}$ , the proton separation energy  $S_p$  is 5.17 MeV and the Coulomb barrier and centrifugal potential for an  $f$ -shell nucleon are approximately 6 MeV and 8 MeV, respectively, and we could see sharp peaks even in the high

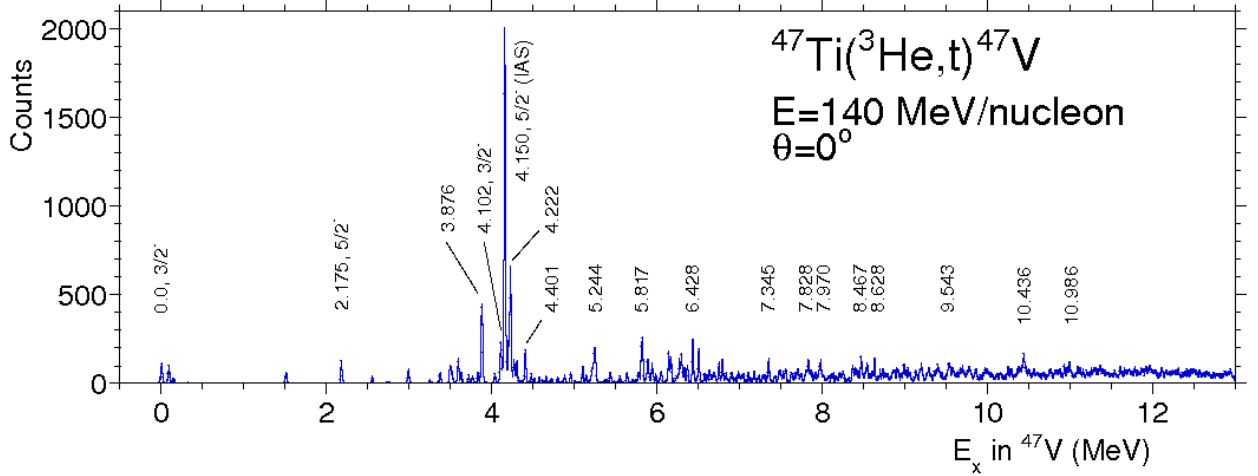


FIG. 1: (Color online) The  $^{47}\text{Ti}(^3\text{He}, t)^{47}\text{V}$  spectrum at  $0^\circ$ . Events with scattering angles  $\Theta \leq 0.5^\circ$  are included. Prominent states populated in  $\Delta L = 0$  transitions are indicated by their excitation energies.

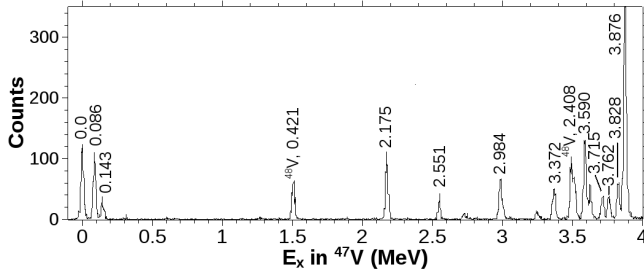


FIG. 2: Part of the  $^{47}\text{Ti}(^3\text{He}, t)^{47}\text{V}$  spectrum shown in Fig. 1 for  $0 \leq E_x \leq 4$  MeV. Prominent states populated in  $\Delta L = 0$  transitions are indicated by their excitation energies. States in  $^{48}\text{V}$  are also indicated.

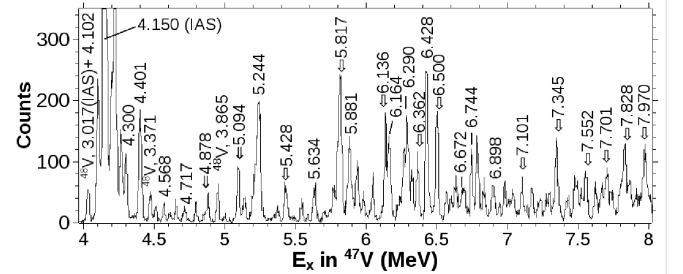


FIG. 3: Part of the  $^{47}\text{Ti}(^3\text{He}, t)^{47}\text{V}$  spectrum shown in Fig. 1 for  $4 \leq E_x \leq 8$  MeV. Prominent states populated in  $\Delta L = 0$  transitions are indicated by their excitation energies. In the region  $E_x \leq 6.7$  MeV, newly observed states that are clearly populated in  $\Delta L = 0$  transitions are indicated by arrows. States of  $^{48}\text{V}$  are also shown.

excitation energy region of the spectrum. The positions of the peaks were obtained by using a peak decomposition program [27]. In order to obtain the peak positions reliably, the peak shape of a well isolated strong peak was used as a reference in the program. From the peak positions obtained, the  $E_x$  values of states in the higher excitation energy region were determined using the well known  $E_x$  values of states in  $^{12}\text{N}$ ,  $^{13}\text{N}$ , and  $^{16}\text{F}$  as references in kinematical calculations. These states were observed in the spectrum from a thin Mylar target with an areal density of  $\approx 1$  mg/cm<sup>2</sup> measured for the purpose of calibration. The measurement was performed under the same conditions as for the  $^{47}\text{Ti}$  target. The  $E_x$  values of the  $^{47}\text{V}$  states could be determined by an interpolation process and they are listed in Tables I-VI. In  $^{47}\text{V}$ , accurate  $E_x$  values of states are known up to 6.8 MeV [28], as shown in Table I and Table II. Most of these  $E_x$  values could be reproduced within a difference of a few keV. In addition the  $E_x$  value of the  $^{12}\text{N}$ , ground state (g.s) which appeared at  $\approx 14.4$  MeV in the  $^{47}\text{V}$  spectrum has been reproduced with an error of 7 keV. Therefore, even if we

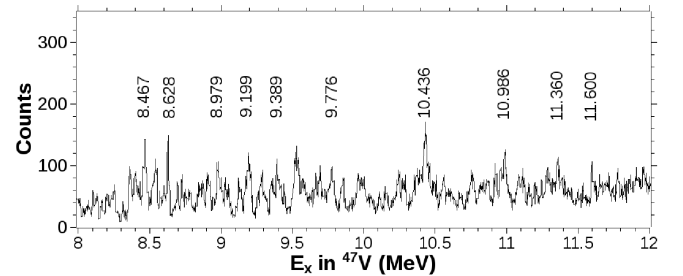


FIG. 4: Part of the  $^{47}\text{Ti}(^3\text{He}, t)^{47}\text{V}$  spectrum shown in Fig. 1 for  $8 \leq E_x \leq 12$  MeV. Prominent states populated in  $\Delta L = 0$  transitions are indicated by their excitation energies.

take the uncertainty of the peak decomposition process into consideration, we believe that the  $E_x$  values of the states listed in Tables I-VI have an accuracy better than 10 keV even in the region above 6.5 MeV.

The intensities of the peaks were obtained up to 12.5 MeV for the  $^{47}\text{V}$  spectra using the peak decomposition program. Above this energy the level density is so high that it is difficult to separate the peaks even with the energy resolution of 20 keV, as we can see in Fig. 1. A continuum background was observed above  $E_x \approx 6.5$  MeV, which increased with excitation energy and appears to be almost saturated at  $E_x \approx 12$  MeV. Accordingly a smooth background was subtracted empirically in the peak fitting analysis.

The main impurity in the target was the  $^{48}\text{Ti}$  isotope, which leads to the observation of states in  $^{48}\text{V}$  in the experimental spectra. In order to identify the  $^{48}\text{V}$  states present in the  $^{47}\text{Ti}(^3\text{He}, t)^{47}\text{V}$  spectra, the  $(^3\text{He}, t)$  spectrum from a target foil enriched in  $^{48}\text{Ti}$  was measured under the same conditions as for the  $^{47}\text{Ti}$  target. Several of the intense peaks assigned to the states in  $^{48}\text{V}$  that were observed as contaminants in the  $^{47}\text{V}$  spectra are indicated in Figs. 2 and 3. Some of the peaks associated with  $^{48}\text{V}$  overlap with peaks in  $^{47}\text{V}$ . Their contributions could be subtracted reliably up to an excitation energy of 7.5 MeV in  $^{47}\text{V}$ . Above this excitation energy, however, the number of  $^{48}\text{V}$  states was large, although most of them were weakly excited. In this energy region, only the contributions from the prominent peaks in  $^{48}\text{V}$  could be subtracted. The peak of the IAS in  $^{48}\text{V}$  is situated at about 50 keV lower energy than the peak of the IAS in  $^{47}\text{V}$  (see Fig. 3). However, due to the good energy resolution in the experiment, the two states could be clearly separated.

In order to distinguish the  $\Delta L = 0$  transitions, the relative intensities of the peaks in the spectra were examined with the angle cuts  $\Theta = 0^\circ - 0.5^\circ$ ,  $0.5^\circ - 0.8^\circ$ ,  $1.2^\circ - 1.6^\circ$ , and  $1.6^\circ - 2.0^\circ$ . It was found that there is no clear enhancement at the larger scattering angles for any of the states strongly excited in the  $\Theta = 0^\circ - 0.5^\circ$  cut, suggesting that they all have  $\Delta L = 0$  character. We assume here that the states populated in  $\Delta L = 0$  transitions, except the IAS, are the GT states [5]. A clear enhancement at larger angles was observed for some of the weakly excited states. This indicates that they have  $\Delta L \geq 1$  character. For the detail of the angular distribution analysis, see Ref. [19].

Some states form close multiplets and the separation of these states in the analysis inevitably has some ambiguity. For these multiplets, the  $\Delta L$  values and the GT strengths were derived for the multiplet as a whole. The multiplets are indicated by the } sign. For some states, a  $\Delta L$  assignment was not possible because of the high level density. Therefore, only the  $E_x$  values are given for these states. In particular in the region above 12 MeV, we could only assign candidates for the states populated in  $\Delta L = 0$  transitions (see Table VI). They are the prominent states seen in the  $0^\circ$  spectrum.

If we think of the simple Shell Model picture, the ground states of the odd mass nuclei  $^{47}\text{Ti}$  and  $^{47}\text{V}$  should have  $J^\pi$  values of  $7/2^-$ . In reality they have the g.s  $J^\pi$  values of  $5/2^-$  and  $3/2^-$ , respectively. These unexpected

$J^\pi$  values are explained by the anomalous  $J$ -coupling of three nucleons [29, 30].

According to the GT selection rules, the  $5/2^-$  g.s of the  $^{47}\text{Ti}$  nucleus can be connected by GT transitions to  $3/2^-$ ,  $5/2^-$ , and  $7/2^-$  states in  $^{47}\text{V}$ . Therefore, the states populated in  $\Delta L=0$  transitions should have one of these spin values. Thus, the g.s of  $^{47}\text{V}$  with  $T_z = +1/2$  and  $J^\pi = 3/2^-$  is populated by a GT transition in the  $^{47}\text{Ti}(^3\text{He}, t)^{47}\text{V}$  reaction. As is seen in Fig. 2, with the energy resolution of 20 keV, one of the best energy resolutions we have ever achieved, the  $^{47}\text{V}$  g.s was well separated from both the nearby  $5/2^-$  state at  $E_x = 86$  keV and the  $7/2^-$  state at 143 keV. It should be noted that the GT transition strength in the  $T_z = +1/2 \rightarrow +3/2$  direction can be studied in the  $\beta^+$ -decay of  $^{47}\text{V}$ , and thus this GT strength can provide a standard  $B(\text{GT})$  value for the purpose of normalization. A  $\log ft$  value of 4.901(5) has been reported for the GT transition from the g.s of  $^{47}\text{V}$  to the g.s of  $^{47}\text{Ti}$  [28]. The  $B(\text{GT})$  values in the direction of the CE-reaction can be derived from this by correcting for the  $(2J+1)$  factors of the spin Clebsch-Gordan coefficients [5]. A  $B(\text{GT})$  value of 0.0319(4) is thus obtained for the  $^{47}\text{Ti}$  g.s  $\rightarrow$   $^{47}\text{V}$  g.s GT transition. The  $B(\text{GT})$  value here is given in units where  $B(\text{GT})=3$  for the  $\beta$  decay of the free neutron.

Many fragmented states were observed up to  $E_x = 12.5$  MeV in the  $^{47}\text{Ti}(^3\text{He}, t)^{47}\text{V}$  reaction. The  $B(\text{GT})$  values of the transitions to these excited states were derived by applying the proportionality given by Eq. (2) to the measured excitation strength of each state.

The gradual decrease in the  $F(q, \omega)$  in Eq. (2) as a function of excitation energy was corrected by using the results of a Distorted Wave Born Approximation (DWBA) calculation. For this purpose, the DW81 code [31] was used assuming that the  $f_{7/2} \rightarrow f_{7/2}$  and  $f_{7/2} \rightarrow f_{5/2}$  configurations were involved. In the calculation, we followed the procedure discussed in Refs. [32–34]. The optical potential parameters were taken from Ref. [35]. The DWBA calculation suggested that the GT cross section decreases with increasing excitation energy, and the decrease was  $\approx 6\%$  from the g.s to  $E_x = 8$  MeV.

In the low-lying  $E_x$  region where the states are clearly separated, in general, the  $\Delta L$  values and also  $B(\text{GT})$  values were well determined. On the other hand, as mentioned, in the highly excited region where the level density was high, the identification of the  $\Delta L$  value, especially for weakly excited states, became difficult. In addition, the close proportionality is in question even for the states populated in  $\Delta L = 0$  transitions [6, 15]. Therefore, for these weakly excited states,  $B(\text{GT})$  values with  $0.005 < B(\text{GT}) < 0.01$  are indicated by the sign “S” and those with  $\leq 0.005$  by “SS” in Tables I - VI. For the states assigned to have  $\Delta L \geq 1$ , the  $B(\text{GT})$  values are not given. Only counts for  $\Theta \leq 0.5^\circ$  are listed.

The uncertainties in the  $B(\text{GT})$  values given in Tables I-VI include the statistical uncertainties in the experimental data, the peak-fit analysis, and also the uncertainty in the  $B(\text{GT})$  value of the g.s–g.s transition

TABLE I: States observed in the  $^{47}\text{Ti}(^3\text{He}, t)^{47}\text{V}$  reaction up to  $E_x = 5.5$  MeV. The  $B(\text{GT})$  values for weak transitions with  $\Delta L = 0$  are listed in two categories marked by S and SS, where S indicates  $0.005 < B(\text{GT}) < 0.01$  and SS indicates  $B(\text{GT}) \leq 0.005$ . The measured counts of states in the  $\Theta \leq 0.5^\circ$  spectrum are listed.

Evaluated values <sup>a</sup>		$(^3\text{He}, t)$ <sup>b</sup>			
$E_x^c$ (MeV)	$J^\pi$	$E_x$ (MeV)	$\Delta L$	Counts	$B(\text{GT})$
0.000	$3/2^-$	0.000	0	1218 ( 49 )	0.0319 ( 4 ) <sup>d</sup>
0.088	$5/2^-$	0.086	0	1012 ( 45 )	0.027 ( 2 )
0.146	$7/2^-$	0.143	0	284 ( 25 )	S
1.139	$7/2^+$	1.141	$\geq 1$	11 ( 5 )	
2.083	$3/2^-$	2.078	$\geq 1$	20 ( 7 )	
2.176	$5/2^-$	2.175	0	994 ( 43 )	0.026 ( 2 )
2.546 (8)	$5/2^-, 7/2^-$	2.551	0	279 ( 32 )	S
2.723	$5/2^-$	2.723	(0)	91 ( 16 )	S
		2.749	$\geq 1$	48 ( 13 )	
2.984	$7/2^-$	2.984	0	603 ( 55 )	0.016 ( 2 )
3.006	$3/2^-$	3.002	0	155 ( 44 )	SS
3.054	$5/2^-$	3.051	$\geq 1$	26 ( 8 )	
3.248	$7/2^-$	3.246	0	119 ( 19 )	SS
3.371	$3/2$	3.372 <sup>e</sup>	0	408 ( 70 )	S
3.517	(5/2)	3.517	0	557 ( 48 )	0.015 ( 1 )
3.590	$5/2$	3.590	0	1330 ( 53 )	0.035 ( 2 )
		3.628	0	467 ( 34 )	0.012 ( 1 )
3.718	$7/2, 5/2, 9/2^+$	3.715	0	386 ( 28 )	0.010 ( 1 )
3.763	$1/2$ to $5/2$	3.762	0	364 ( 29 )	0.010 ( 1 )
3.823	$1/2, 3/2$	3.828	0	458 ( 33 )	0.012 ( 1 )
3.876	(5/2), $3/2^-$ or $7/2$	3.876	0	4191 ( 90 )	0.112 ( 5 )
		4.032	0	504 ( 32 )	0.013 ( 1 )
4.100	$3/2^-$	4.102 <sup>e</sup>	0	716 ( 124 )	0.019 ( 3 )
4.150 <sup>f</sup>	$5/2(-)$	4.150	0	17309 ( 185 ) <sup>g</sup>	
			0	2863 ( 821 ) <sup>h</sup>	0.073 ( 21 )
4.197	$5/2$	4.198	0	1611 ( 104 )	0.043 ( 3 )
4.222	$5/2$	4.222	0	5690 ( 136 )	0.152 ( 7 )
		4.266	0	1122 ( 58 )	0.030 ( 2 )
4.296 (12)	(7/2) <sup>-</sup>	4.300	0	1071 ( 51 )	0.029 ( 2 )
4.403	$7/2, 5/2, 9/2$	4.401	0	1734 ( 58 )	0.046 ( 2 )
4.510	$5/2, 3/2^-$	4.511	$\geq 1$	258 ( 25 )	
4.569	$5/2$	4.568	0	231 ( 22 )	S
4.613 (20)		4.613	$\geq 1$	155 ( 20 )	
		4.654	0	299 ( 25 )	S
4.719	$3/2, 1/2, 5/2^-$	4.717	(0)	280 ( 24 )	S
4.797	$3/2, 1/2^-, 5/2^-$	4.796	0	299 ( 24 )	S
4.853	$5/2, 1/2^-, 3/2^-$	4.848	$\geq 1$	79 ( 17 )	
		4.878	0	407 ( 31 )	0.011 ( 1 )
4.999	$5/2, 7/2$	4.998	$\geq 1$	105 ( 17 )	
4.999		5.094	0	742 ( 39 )	0.020 ( 1 )
5.142	$3/2, 1/2^-, 5/2^-$	5.137	0	399 ( 32 )	0.011 ( 1 )
		5.206	0	635 ( 85 )	0.017 ( 2 )
5.223	$3/2, 5/2^-$	5.228 } 5.244 }	0	2657 ( 173 )	0.071 ( 5 )
5.244(20)	$1/2^-, 3/2^+$	5.373	$\geq 1$	194 ( 26 )	
		5.428	0	518 ( 61 )	0.014 ( 2 )
		5.544 <sup>e</sup>	0	105 ( 41 )	SS

<sup>a</sup>From Ref. [28].

<sup>b</sup>Present work.

<sup>c</sup>Energy uncertainties of  $< 1$  keV are not indicated.

<sup>d</sup>From  $\beta$ -decay measurement.

<sup>e</sup>The contribution from the  $^{48}\text{V}$  state was subtracted.

<sup>f</sup>The IAS ( $T = 3/2$ ).

<sup>g</sup>The total count of the IAS.

<sup>h</sup>Estimated count corresponding to the GT transition strength in the IAS.



that was measured in the  $^{47}\text{V}$ ,  $\beta$  decay. However, the uncertainties associated with the background subtraction were not included. Therefore, the  $B(\text{GT})$  values of the states in the highly excited region, where the background counts were larger, can have larger uncertainties than is indicated.

The 4.150 MeV state is the IAS of the g.s of  $^{47}\text{Ti}$ . In the  $T_z = +3/2 \rightarrow +1/2$ , CE reaction, both the Fermi strength and the GT strength contribute in the transition to the IAS. In order to derive the  $B(\text{GT})$  strength in the transitions to the IAS, we introduce the ratio of GT and Fermi unit cross-sections denoted as  $R^2$  [7] and defined by

$$R^2 = \frac{\hat{\sigma}_{\text{GT}}(0^\circ)}{\hat{\sigma}_{\text{F}}(0^\circ)} = \frac{\sigma_{\text{GT}}(0^\circ)}{B(\text{GT})} \bigg/ \frac{\sigma_{\text{F}}(0^\circ)}{B(\text{F})}, \quad (3)$$

where we assume that all of the Fermi transition strength is concentrated in the IAS, and it consumes the complete sum rule value of  $B(\text{F}) = N - Z = 3$ . We also assume that  $R^2$  is a constant for a given mass number  $A$  and is a smooth function of  $A$ . The  $A$  dependence of  $R^2$  was systematically studied and a smooth increase in  $R^2$  was observed as  $A$  increases [36, 37]. A value of  $R^2 = 8.1 \pm 0.4$  can be deduced for the  $A = 47$  nuclei by quadratically interpolating the experimentally obtained  $R^2$  values for  $A = 26$  [13], 34 [15], 46 [16], 54 [18], 64 [19], 78 [38], 118, and 120 [39]. The resulting  $B(\text{GT})$  value obtained for the GT transition to the  $E_x = 4.150$  MeV, IAS is shown in Table I.

## IV. RESULTS AND DISCUSSION

### A. $B(\text{GT})$ distribution in $^{47}\text{V}$

Many discrete states, including weakly excited states, could be studied up to  $E_x = 12.5$  MeV. Some concentrations of GT strength were found around 4 MeV and 6 MeV, but in general, the GT strength was highly fragmented, and no compact resonance structure of GT strength was observed [see Fig. 5(a)].

Shell model (SM) calculations in the full  $pf$ -shell model space are now available. The experimental  $B(\text{GT})$  distribution in  $^{47}\text{V}$  up to  $E_x = 12$  MeV is compared with the results of the SM calculation using the GXPf1 interaction [42] [Fig. 5(b)]. The  $B(\text{GT})$  values from the SM calculation include the average normalization factor (quenching factor) of  $(0.74)^2$  [43]. It is seen that the experimental and calculated  $B(\text{GT})$  distributions are generally in agreement. The fragmentation of states, although more pronounced in the experimental distribution, is also relatively well reproduced. However, the order of the  $J$  values for the lowest three states is different from that of evaluated values [28]; in the SM calculation, they were in the order of  $J=5/2$ ,  $3/2$ , and  $7/2$  while the evaluated values were  $J=3/2$ ,  $5/2$ , and  $7/2$ . Separate calculations using the interaction KB3G [44] in the  $pf$

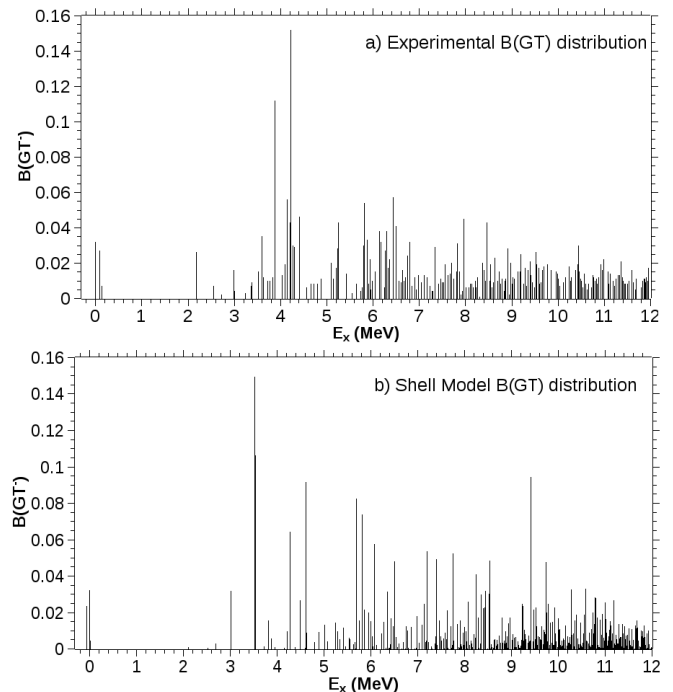


FIG. 5: A comparison of the experimental and theoretical  $B(\text{GT})$  strength distributions with (a) the  $B(\text{GT})$  distribution derived from the  $^{47}\text{Ti}(^3\text{He}, t)^{47}\text{V}$  measurement, and (b) the  $B(\text{GT})$  distribution from the Shell Model (SM) calculation.

model space and the program NuSHELL [45] gave essentially the same results.

The good agreement between experiment and theory can also be seen in the cumulative sum of the  $B(\text{GT})$  values as a function of excitation energy shown in Fig. 6. The cumulative  $B(\text{GT})$  strength increases very gradually as a function of excitation energy in both experiment and the SM calculations. This gentle increase shows that the GT strength is fragmented over the whole region up to 12.5 MeV, where we had to stop the analysis due to the high level density of states. Above 10 MeV, the SM cumulative sum is larger than the experimental one. In the  $(^3\text{He}, t)$  experiment on  $^{54}\text{Fe}$ , a similar tendency was observed for the GT strength distribution in  $^{54}\text{Co}$  [18].

### B. Total $B(\text{GT})$ strength

The total sum of the  $B(\text{GT})$  strength observed in the excitation of discrete states was 3.60. We suggest that this  $B(\text{GT})$  value is the minimum of the total sum in the entire region up to 12.5 MeV. One can see that this value is only 40% of the sum-rule-limit value of  $3(N - Z)$  even if the negative contribution from the GT strengths in the  $\beta^+$  direction is ignored.

A continuum from quasifree scattering (QFS) [40, 41] is expected above the proton separation energy of  $S_p = 5.17$

TABLE II: States observed in the  $^{47}\text{Ti}(^3\text{He}, t)^{47}\text{V}$  reaction between  $E_x = 5.5$  and 7.7 MeV. For details, see the caption to Table I.

Evaluated values <sup>a</sup>		$(^3\text{He}, t)$ <sup>b</sup>			
$E_x^c$ (MeV)	$J^\pi$	$E_x$ (MeV)	$\Delta L$	Counts	$B(\text{GT})$
5.585 (12)	$1/2^-, 3/2^-$	5.587	$(\geq 1)$	60 ( 15 )	
5.635	$3/2^-$	5.634 <sup>d</sup>	0	307 ( 41 )	S
		5.703	$(\geq 1)$	156 ( 23 )	
5.738 (3)	$1/2, 3/2$	5.739	(0)	140 ( 26 )	SS
		5.770 <sup>d</sup>	(0)	215 ( 64 )	S
		5.803 } 5.817 }	0	3123 ( 164 )	0.084 ( 5 )
5.885	$3/2$	5.881 } 5.898 }	0	1514 ( 151 )	0.041 ( 4 )
5.895	$1/2$	5.933	0	820 ( 99 )	0.022 ( 3 )
5.928 (20)		5.982	0	367 ( 36 )	0.010 ( 1 )
		6.046	0	536 ( 41 )	0.015 ( 1 )
		6.136	0	1406 ( 68 )	0.038 ( 2 )
6.166	$3/2^{(-)}$	6.164	0	1187 ( 62 )	0.032 ( 2 )
		6.241	(0)	215 ( 26 )	S
6.271	$(3/2)$	6.266	0	982 ( 87 )	0.027 ( 3 )
6.297	$3/2^{(-)}$	6.290	0	1397 ( 82 )	0.038 ( 3 )
		6.322	0	641 ( 48 )	0.017 ( 1 )
		6.362	0	792 ( 45 )	0.022 ( 2 )
6.426 or 6.427	$(3/2)$ or $(5/2)$	6.428	0	2099 ( 66 )	0.057 ( 3 )
		6.500	0	1504 ( 133 )	0.041 ( 4 )
		6.567	0	368 ( 35 )	0.010 ( 1 )
		6.600	(0)	313 ( 38 )	S
		6.632	0	578 ( 43 )	0.016 ( 1 )
6.680	$7/2^{(-)}$	6.672 } 6.693 }	(0)	795 ( 54 )	0.022 ( 2 )
6.749 (20)		6.744	0	869 ( 47 )	0.024 ( 2 )
		6.787	0	1157 ( 54 )	0.032 ( 2 )
		6.834 <sup>d</sup>	0	249 ( 51 )	S
6.895 (20)		6.898 <sup>d</sup>	0	437 ( 43 )	0.012 ( 1 )
		6.941	0	184 ( 27 )	SS
		6.979	0	468 ( 45 )	0.013 ( 1 )
		7.000 } 7.018 }	$\geq 1$	341 ( 26 )	
		7.040 <sup>d</sup>	0	330 ( 54 )	S
		7.101	0	463 ( 41 )	0.013 ( 1 )
		7.128	$\geq 1$	125 ( 20 )	
		7.172	0	443 ( 37 )	0.012 ( 1 )
		7.212	$\geq 1$	97 ( 46 )	
		7.231	0	243 ( 50 )	S
		7.272 <sup>d</sup>		156 ( 50 )	SS
		7.294 <sup>d</sup>		163 ( 48 )	SS
		7.345 <sup>d</sup>	0	1041 ( 79 )	0.032 ( 2 )
		7.424	(0)	300 ( 33 )	S
		7.471 } 7.491 }	0	730 ( 68 )	0.020 ( 2 )
		7.523	0	312 ( 44 )	S
		7.552	0	699 ( 49 )	0.019 ( 2 )
		7.623	0	455 ( 40 )	0.013 ( 1 )
		7.668	0	498 ( 44 )	0.014 ( 1 )
		7.701	0	707 ( 50 )	0.020 ( 2 )
		7.738	0	392 ( 40 )	0.011 ( 1 )

<sup>a</sup>From Ref. [28].

<sup>b</sup>Present work.

<sup>c</sup>Energy uncertainties of  $< 1$  keV are not indicated.

<sup>d</sup>The contribution from the  $^{48}\text{V}$  state was subtracted.



TABLE III: States observed in the  $^{47}\text{Ti}(^3\text{He}, t)^{47}\text{V}$  reaction between  $E_x = 7.8$  and 9.6 MeV. For details, see the caption to Table I.

$(^3\text{He}, t)^a$			
$E_x$ (MeV)	$\Delta L$	Counts	$B(\text{GT})$
7.799	0	548 ( 49 )	0.015 ( 2 )
7.828	0	1132 ( 64 )	0.031 ( 2 )
7.863	0	555 ( 47 )	0.015 ( 1 )
7.906 <sup>b</sup>	(0)	88 ( 57 )	SS
7.933	0	154 ( 50 )	SS
7.970	0	1610 ( 124 )	0.045 ( 4 )
8.007	0	203 ( 46 )	S
8.071	0	217 ( 36 )	S
8.106	0	296 ( 51 )	S
8.128	0	277 ( 49 )	S
8.168	0	206 ( 34 )	S
8.204	0	364 ( 46 )	0.010 ( 1 )
8.231	0	230 ( 62 )	S
8.251	0	429 ( 59 )	0.012 ( 2 )
8.313 <sup>b</sup>	(0)	30 ( 50 )	SS
8.366	0	708 ( 49 )	0.020 ( 2 )
8.399 <sup>b</sup>	0	564 ( 59 )	0.016 ( 2 )
8.426	(0)	356 ( 53 )	0.010 ( 2 )
8.467	0	1529 ( 98 )	0.043 ( 3 )
8.520 <sup>b</sup>	0	353 ( 62 )	0.010 ( 2 )
8.542 <sup>b</sup>	0	678 ( 72 )	0.019 ( 2 )
8.577	(0)	230 ( 50 )	S
8.600	0	320 ( 54 )	S
8.628	0	826 ( 54 )	0.023 ( 2 )
8.695	0	365 ( 57 )	0.010 ( 2 )
8.728	(0)	522 ( 52 )	0.015 ( 2 )
8.755	0	277 ( 49 )	S
8.783	0	382 ( 45 )	0.011 ( 1 )
8.829	0	157 ( 62 )	SS
8.850 <sup>b</sup>	0	756 ( 92 )	0.021 ( 3 )
8.871 <sup>b</sup>			
8.913 <sup>b</sup>	0	991 ( 144 )	0.028 ( 4 )
8.948 <sup>b</sup>	(0)	60 ( 35 )	SS
8.979	0	727 ( 68 )	0.020 ( 2 )
9.001 <sup>b</sup>	(0)	299 ( 67 )	S
9.030	0	439 ( 57 )	0.012 ( 2 )
9.055	0	376 ( 50 )	0.011 ( 1 )
9.130	0	536 ( 45 )	0.015 ( 1 )
9.175	0	515 ( 58 )	0.015 ( 2 )
9.199	0	880 ( 63 )	0.025 ( 2 )
9.259	(0)	297 ( 47 )	S
9.286	0	604 ( 63 )	0.017 ( 2 )
9.311	(0)	251 ( 48 )	S
9.357	0	559 ( 50 )	0.016 ( 2 )
9.389	0	731 ( 69 )	0.021 ( 2 )
9.412	(0)	452 ( 64 )	0.013 ( 2 )
9.444	(0)	336 ( 43 )	S
9.497	0	204 ( 50 )	S
9.522 <sup>b</sup>	0	1585 ( 96 )	0.045 ( 3 )
9.543 <sup>b</sup>			
9.576	(0)	594 ( 60 )	0.017 ( 2 )
9.601	(0)	279 ( 52 )	S

<sup>a</sup>Present work.

<sup>b</sup>The contribution from the  $^{48}\text{V}$  state was subtracted.

TABLE IV: States observed in the  $^{47}\text{Ti}(^3\text{He}, t)^{47}\text{V}$  reaction between  $E_x = 9.6$  and 11.3 MeV. For details, see the caption to Table I.

$(^3\text{He}, t)^a$			
$E_x$ (MeV)	$\Delta L$	Counts	$B(\text{GT})$
9.634	0	318 ( 48 )	S
9.663	(0)	552 ( 56 )	0.016 ( 2 )
9.693	0	650 ( 58 )	0.018 ( 2 )
9.723	$\geq 1$	320 ( 50 )	
9.752	$\geq 1$	373 ( 65 )	
9.776	0	674 ( 87 )	0.019 ( 3 )
9.797	( $\geq 1$ )	234 ( 66 )	
9.852	0	564 ( 60 )	0.016 ( 2 )
9.909	$\geq 1$	166 ( 37 )	
9.937	( $\geq 1$ )	152 ( 53 )	
9.960	0	527 ( 70 )	0.015 ( 2 )
9.984 <sup>b</sup>	(0)	869 ( 73 )	0.025 ( 2 )
10.007 <sup>b</sup>			
10.036	(0)	246 ( 57 )	S
10.060	( $\geq 1$ )	203 ( 48 )	
10.111	0	318 ( 40 )	S
10.156	0	420 ( 43 )	0.012 ( 1 )
10.207	$\geq 1$	228 ( 40 )	
10.241	0	622 ( 56 )	0.018 ( 2 )
10.271 <sup>b</sup>	(0)	795 ( 74 )	0.022 ( 2 )
10.291 <sup>b</sup>			
10.351	( $\geq 1$ )	303 ( 87 )	
10.371	(0)	571 ( 101 )	0.016 ( 3 )
10.397	( $\geq 1$ )	553 ( 101 )	
10.421 <sup>b</sup>	(0)	1702 ( 177 )	0.049 ( 5 )
10.436 <sup>b</sup>			
10.460	(0)	512 ( 95 )	0.015 ( 3 )
10.489 <sup>b</sup>	(0)	735 ( 83 )	0.021 ( 2 )
10.508 <sup>b</sup>			
10.541 <sup>b</sup>	(0)	704 ( 90 )	0.020 ( 3 )
10.561 <sup>b</sup>			
10.590	(0)	275 ( 74 )	S
10.611	( $\geq 1$ )	255 ( 79 )	
10.634		172 ( 57 )	
10.667	(0)	265 ( 69 )	S
10.725	(0)	224 ( 54 )	S
10.750 <sup>b</sup>	(0)	850 ( 94 )	0.025 ( 3 )
10.769 <sup>b</sup>			
10.807	0	342 ( 65 )	0.010 ( 2 )
10.830	0	390 ( 89 )	0.011 ( 3 )
10.853 <sup>b</sup>	(0)	704 ( 103 )	0.020 ( 3 )
10.873 <sup>b</sup>			
10.925	0	649 ( 50 )	0.019 ( 2 )
10.960	0	537 ( 59 )	0.016 ( 2 )
10.986	0	769 ( 138 )	0.022 ( 4 )
11.005	( $\geq 1$ )	340 ( 136 )	
11.083	0	505 ( 90 )	0.015 ( 3 )
11.102 <sup>b</sup>	(0)	752 ( 136 )	0.022 ( 4 )
11.121 <sup>b</sup>			
11.157	( $\geq 1$ )	378 ( 47 )	
11.196 <sup>b</sup>	(0)	568 ( 61 )	0.017 ( 2 )
11.216 <sup>b</sup>			
11.247	(0)	374 ( 48 )	0.011 ( 1 )
11.280	( $\geq 1$ )	558 ( 73 )	

<sup>a</sup>Present work.

TABLE V: States observed in the  $^{47}\text{Ti}(^3\text{He}, t)^{47}\text{V}$  reaction between  $E_x = 11.3$  and 12.0 MeV. For details, see the caption to Table I.

$(^3\text{He}, t)^a$			
$E_x$ (MeV)	$\Delta L$	Counts	$B(\text{GT})$
11.302	(0)	454 ( 75 )	0.013 ( 2 )
11.330	(0)	443 ( 62 )	0.013 ( 2 )
11.360	0	737 ( 71 )	0.021 ( 2 )
11.387		405 ( 79 )	
11.409		334 ( 83 )	
11.433		278 ( 77 )	
11.456		288 ( 61 )	
11.501		261 ( 40 )	
11.538	(0)	325 ( 45 )	0.010 ( 1 )
11.600	0	547 ( 63 )	0.016 ( 2 )
11.624	(0)	297 ( 62 )	S
11.653	( $\geq 1$ )	395 ( 68 )	
11.669	(0)	168 ( 58 )	SS
11.691		378 ( 68 )	
11.715	$\geq 1$	468 ( 66 )	
11.746	( $\geq 1$ )	326 ( 50 )	
11.778	$\geq 1$	536 ( 77 )	
11.800	(0)	208 ( 97 )	S
11.824	(0)	345 ( 86 )	0.010 ( 3 )
11.852 } 11.872 }	(0)	751 ( 115 )	0.022 ( 3 )
11.896 } 11.914 } 11.934 }	(0)	1067 ( 171 )	0.030 ( 5 )
11.959	(0)	583 ( 100 )	0.017 ( 3 )
11.983	$\geq 1$	419 ( 107 )	

<sup>a</sup>Present work.

TABLE VI: Candidates for the states populated in  $\Delta L = 0$  transitions and observed in the  $^{47}\text{Ti}(^3\text{He}, t)^{47}\text{V}$  reaction between  $E_x = 12.0$  and 12.5 MeV. For details, see the caption to Table I.

$(^3\text{He}, t)^a$			
$E_x$ (MeV)	$\Delta L$	Counts	$B(\text{GT})$
12.103	(0)	469 ( 99 )	0.014 ( 3 )
12.158	(0)	384 ( 53 )	0.011 ( 2 )
12.186	(0)	296 ( 74 )	S
12.229 } 12.251 } 12.273 }	(0)	892 ( 109 )	0.026 ( 3 )
12.304	0	456 ( 51 )	0.014 ( 2 )
12.387	(0)	246 ( 87 )	S
12.415 } 12.433 }	(0)	625 ( 114 )	0.018 ( 3 )
12.460 } 12.476 } 12.497 }	(0)	910 ( 98 )	0.026 ( 3 )

<sup>a</sup>Present work.

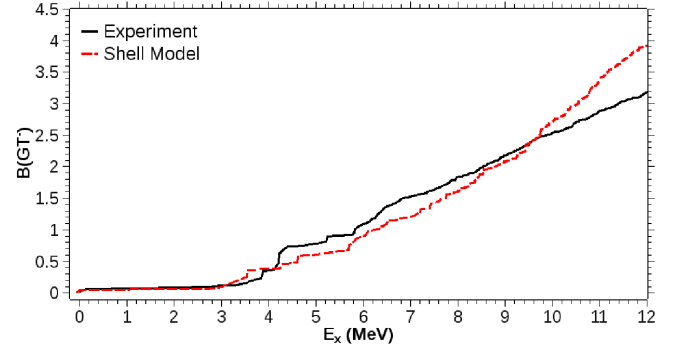


FIG. 6: (Color online) A comparison of the summed  $B(\text{GT})$  strengths from the  $^{47}\text{Ti}(^3\text{He}, t)^{47}\text{V}$  measurement (solid line) and the SM calculation using the GXPF1 interaction (dotted line) as a function of excitation energy.

MeV. Since there is no theory for reliably calculating the cross section of the QFS continuum, a background described by a smooth line was subtracted in our analysis, as mentioned above. Under the extreme assumption that all of the counts in the continuum are due to GT transitions, they would add additional value of 1.58 to the summed  $B(\text{GT})$  strength in the region up to 12.5 MeV. Therefore, our result shows that the total sum of the  $B(\text{GT})$  strength located in the energy region from 0 to 12.5 MeV is  $\approx 40\%$ , but can never be more than 57% of the sum-rule-limit value.

### C. $M1$ $\gamma$ transitions in $^{47}\text{V}$

The  $M1$   $\gamma$  transitions from the IAS at  $E_x = 4.150$  MeV to low-lying states in  $^{47}\text{V}$  are analogous to the corresponding GT transitions to the same low-lying states observed in the  $^{47}\text{Ti}(^3\text{He}, t)^{47}\text{V}$  reaction, as shown in Fig. 7.

In order to compare the strengths of analogous  $M1$  and GT transitions, we have to examine the similarities and differences between these transitions. The GT operator has only an isovector (IV) spin ( $\sigma\tau$ ) term. The GT transition strength  $B(\text{GT})$  reduced in isospin [5, 46] is given by

$$B(\text{GT}) = \frac{1}{(2J_i + 1)} \frac{1}{2} \frac{C_{\text{GT}}^2}{(2T_f + 1)} [M_{\text{GT}}(\sigma\tau)]^2, \quad (4)$$

where  $C_{\text{GT}}$  is the isospin Clebsch-Gordan (CG) coefficient  $(T_i T_{zi} 1 \pm 1 | T_f T_{zf})$  with  $T_{zf} = T_{zi} \pm 1$ . The matrix element  $M_{\text{GT}}(\sigma\tau)$  denotes the GT transition matrix element of  $\sigma\tau$  type.

In addition to the IV spin ( $\sigma\tau$ ) term, the  $M1$  operator has an IV orbital ( $\ell\tau$ ) term and an isoscalar (IS) term. Since the  $M1$  transitions of interest here are between the  $T = 3/2$ , IAS and the  $T = 1/2$  states populated in GT transitions, only the IV terms can contribute. Then, the  $M1$  transition strength  $B(M1)$  reduced in isospin [5, 46]

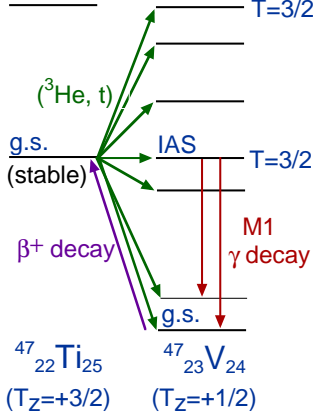


FIG. 7: (Color online) Schematic view of the isospin analog states and analogous transitions in the  $A = 47$ ,  $T_z = +3/2$  and  $+1/2$  isobaric system. The Coulomb displacement energies are removed so that the isospin symmetry of the states and transitions becomes clearer. The type of the reaction or decay is shown alongside the arrow indicating the transition.

is given by

$$B(M1) = \frac{1}{(2J_i + 1)} \frac{3}{4\pi} \mu_N^2 \frac{C_{M1}^2}{(2T_f + 1)} \times \left[ g_\ell^{\text{IV}} M_{M1}(\ell\tau) + g_s^{\text{IV}} \frac{1}{2} M_{M1}(\sigma\tau) \right]^2, \quad (5)$$

where  $C_{M1}$  expresses the isospin CG coefficient ( $T_i T_{zi} 10 | T_f T_{zf}$ ) with  $T_{zf} = T_{zi}$ . The matrix elements  $M_{M1}(\sigma\tau)$  and  $M_{M1}(\ell\tau)$  denote the  $\sigma\tau$ -type and  $\ell\tau$ -type components of the  $M1$  transition matrix element, respectively. The IV combinations of spin and orbital  $g$  factors are expressed by  $g_s^{\text{IV}} = \frac{1}{2}(g_s^\pi - g_s^\nu)$  and  $g_\ell^{\text{IV}} = \frac{1}{2}(g_\ell^\pi - g_\ell^\nu)$ , respectively. Using the bare spin and orbital  $g$  factors of protons and neutrons, i.e.,  $g_s^\pi = 5.586$ ,  $g_s^\nu = -3.826$  and  $g_\ell^\pi = 1$ ,  $g_\ell^\nu = 0$ , we get  $g_s^{\text{IV}} = 4.706$  and  $g_\ell^{\text{IV}} = 0.5$ . Due to the large value of the coefficient  $g_s^{\text{IV}}$ , it is expected that the  $\sigma\tau$  term is usually larger than the  $\ell\tau$  term [47, 48]. Therefore, the strengths for the analogous GT and  $M1$  transitions are expected to correspond (for details see, e.g., Ref. [46]).

The energies  $E_\gamma$  and relative intensities  $I_\gamma$  of the  $\gamma$  transitions from the IAS to the states at  $E_x = 0.0, 0.088$ , and  $0.146$  MeV are given in Ref. [28] and are listed in columns 3 and 4 of Table VII, respectively. Using these values, the transition strengths proportional to the  $M1$  transition strengths  $B(M1)$  can be deduced under the assumption that the  $E2/M1$  mixing ratios  $\delta$  are small for these transitions. They are obtained using the relationship (see, e.g., Ref. [49])

$$B(M1) \propto \frac{1}{E_\gamma^3} I_\gamma. \quad (6)$$

The relative strengths of the  $B(M1)$  values for these three  $M1$  transitions are listed in column 5 of Table VII,

and the relative strengths for the corresponding GT transitions are given in column 7, where the strongest  $M1$  and GT strengths to the g.s. of  $^{47}\text{V}$  are normalized to unity. As one can see, the intensity ratios of the analogous  $M1$  and GT transitions are in good agreement. From the similarity of these ratios, we see that the contributions of the  $\ell\tau$  term in the transitions are relatively small.

As discussed in Refs. [12, 50, 51] it was found that the contributions of  $\ell\tau$  terms are very large for the deformed nuclei in the  $A = 23 - 25$  mass region, where large enhancements or suppressions of  $M1$  strengths compared to the analogous GT transition strengths were observed. Therefore, it is suggested that the deformation of  $^{47}\text{V}$  is small, which is in good agreement with the result of a macroscopic calculation for the nuclear deformation of  $^{47}\text{V}$  saying that the deformation parameter  $\beta_2$  is zero [52].

#### D. $T_z = +3/2$ to $T_z = +1/2$ GT transitions

It is interesting to compare the spectrum obtained in the present  $^{47}\text{Ti}(^3\text{He}, t)^{47}\text{V}$  reaction study with the spectrum from another  $T_z = +3/2 \rightarrow T_z = +1/2$  case. In Fig. 8, our  $0^\circ$  spectrum is compared with the  $^{41}\text{K}(^3\text{He}, t)^{41}\text{Ca}$  spectrum obtained at  $0^\circ$  and at the same incoming energy of 140 MeV/nucleon at RCNP [53]. The scales of the ordinates are adjusted so that the states populated with the same  $B(\text{GT})$  value have the same height in these two spectra.

We can try to understand the difference in the strength distributions in simple terms. In  $^{41}\text{K}$ , we begin with a proton hole in the  $d_{3/2}$  orbital and two neutrons in the  $f_{7/2}$  orbital. The g.s. of  $^{47}\text{Ti}$  has two protons in the  $f_{7/2}$  orbital and five neutrons in the  $f_{7/2}$  orbital. Accordingly, in the  $(^3\text{He}, t)$  reaction on  $^{41}\text{K}$ , GT transitions mainly proceed from the neutron ( $\nu$ )  $f_{7/2}$  orbital to the proton ( $\pi$ )  $f_{7/2}$  and  $\pi f_{5/2}$  orbitals. This results in states in  $^{41}\text{Ca}$  of particle-particle ( $p-p$ ) character, namely  $\pi f_{7/2} - \nu f_{7/2}$  and  $\pi f_{5/2} - \nu f_{7/2}$  configurations on top of the  $^{40}\text{Ca}$  core with one  $\pi d_{3/2}$  hole. Because of the attractive nature of the  $p-p$  interaction [54], we expect that these states to lie at a relatively low excitation energy.

Turning to the GT transitions starting from the  $^{47}\text{Ti}$  g.s., we also find that the transitions with  $\nu f_{7/2} \rightarrow \pi f_{7/2}$  and  $\nu f_{7/2} \rightarrow \pi f_{5/2}$  are involved. However, the resulting states in  $^{47}\text{V}$  are not of  $p-p$  character, but rather of particle-hole ( $p-h$ ) character. Since the  $p-h$  interaction is of repulsive nature [54], the states observed are pushed up in excitation energy, as can be seen in Fig. 8. A very similar comparison has been made for the strength distributions of GT transitions starting from  $T_z = +1$  nuclei in the  $pf$ -shell [5].

TABLE VII: Comparison of analogous GT and  $M1$  transitions in the  $A = 47$  isobars. The  $\gamma$  transitions in  $^{47}\text{V}$  from the 4.150 MeV, IAS to lower-lying states are analogous to the GT transitions to the same low-lying states from the g.s. of  $^{47}\text{V}$ . Relative transition strengths can be compared for these transitions assuming that the  $\gamma$  transitions are of pure  $M1$  nature.

States in $^{47}\text{V}$		$\gamma$ transitions in $^{47}\text{V}$			GT transitions to $^{47}\text{V}$	
$E_x$ (MeV) <sup>a</sup>	$2J^\pi$ <sup>a</sup>	$E_\gamma$ (MeV)	Intensity ratio <sup>a</sup>	$B(M1)$ ratio	$B(\text{GT})$ <sup>b</sup>	$B(\text{GT})$ ratio
0.0	$3^-$	4.150	50(1)	1.00(2)	0.0319(4)	1.00(1)
0.088	$5^-$	4.063	37(1)	0.79(3)	0.027(2)	0.81(13)
0.146	$7^-$	4.004	13(1)	0.29(2)	0.007(2)	0.22(6)

<sup>a</sup>From Ref. [28].

<sup>b</sup>Present work.

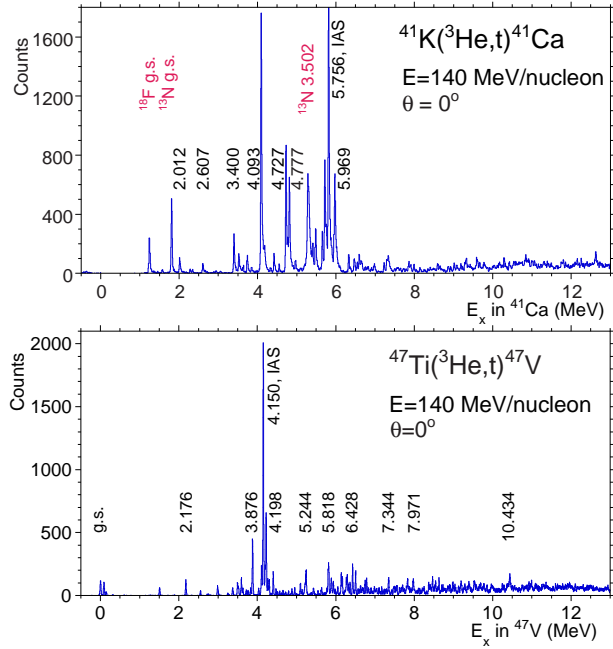


FIG. 8: (Color online) Comparison of (a) the  $^{41}\text{K}(^3\text{He},t)^{41}\text{Ca}$  spectrum and (b) the  $^{47}\text{Ti}(^3\text{He},t)^{47}\text{V}$  spectrum measured at 140 MeV/nucleon and  $0^\circ$ . The scales of the ordinates are adjusted so that the states with the same  $B(\text{GT})$  value have the same height in these two spectra.

## V. SUMMARY

The  $T_z = +3/2 \rightarrow +1/2$ , GT transitions were studied in the  $^{47}\text{Ti}(^3\text{He},t)^{47}\text{V}$  reaction at the intermediate beam energy of 140 MeV/nucleon and  $0^\circ$  scattering angle. An energy resolution of 20 keV was achieved. This was one of the best resolutions that has ever been achieved at this incoming beam energy of 420 MeV in total. Owing to this excellent energy resolution many discrete states, including those weakly excited, could be studied up to 12.5 MeV. As a result of angular distribution analysis, it was found that  $\Delta L = 0$  strengths, most probably GT strengths, were highly fragmented. There were some concentrations around  $E_x = 4$  and 6 MeV, but no strong

concentration of the strength was observed. In addition, judging from the increasing trend of the cumulative sum of the  $B(\text{GT})$  strength, it seems that the strength still exists even in the region above 12.5 MeV.

Shell model calculations were performed using the GXPf1 interaction. The experimental  $B(\text{GT})$  distribution was well reproduced, although a higher degree of fragmentation was observed in the experimental distribution.

The strengths of  $M1$  transitions in  $^{47}\text{V}$  from the IAS to the three low-lying states were compared with the analogous transitions observed in the  $^{47}\text{Ti}(^3\text{He},t)^{47}\text{V}$  reaction. It was found that the ratios of  $M1$  and GT strengths are in good agreement.

A comparison was made for  $T_z = +3/2 \rightarrow +1/2$ , GT transitions starting from the nuclei  $^{41}\text{K}$  and  $^{47}\text{Ti}$ . In the  $^{41}\text{K}(^3\text{He},t)^{41}\text{Ca}$  spectrum, the GT strengths are concentrated in the region between 4 – 6 MeV, while in the  $^{47}\text{Ti}(^3\text{He},t)^{47}\text{V}$  spectrum, they are spread out in energy.

We note that the  $T_z = -3/2 \rightarrow -1/2$ , GT transition strengths, i.e., the GT transition strengths that can be observed in the  $^{47}\text{Mn} \rightarrow ^{47}\text{Cr}$ ,  $\beta^+$  decay [55], can be deduced from the accurate measurement of analogous GT transitions in the high resolution study of the  $(^3\text{He},t)$  reaction, if the isospin symmetry [5, 56] of the  $T_z = \pm 3/2 \rightarrow \pm 1/2$ , analogous GT transitions is assumed. It should be stressed that the study of GT transition strengths starting from an exotic nucleus, such as  $^{47}\text{Mn}$ , contributes to the understanding of weak processes that are important in astrophysics and have not been well studied previously.

## VI. ACKNOWLEDGMENTS

The authors would like to thank the accelerator group of RCNP, Osaka, where the high-resolution  $(^3\text{He},t)$  experiment was performed under the experimental program No. E307. EG and GS acknowledge the support of the Turkish Atomic Energy Authority (TAEK) under Project No. CERN-A5.H2.H1.01-4. EG acknowledges the support of the Istanbul University Scientific Research Projects Coordination Unit (BAP) under Project

Nos. NP-5626, UDP 7732 and UDP 26540 and thanks Prof. B. Akkus for encouragement and Prof. W. Gelletly (Surrey) for discussions during the preparation of this paper. YF acknowledges the support of MEXT, Japan under Grant Nos. 18540270 and 22540310, BR, AA and EEA the support of Spanish Ministry under Grant Nos.

FPA2005-03993, FPA2008-06419-C02-01, and FPA2011-24553 and RGTZ, JD, CJG, RM, and GP the support of US NSF under Grant Nos. PHY-0606007 and PHY-0822648(JINA). YF and BR acknowledge support of Japan-Spain collaboration program by JSPS and CSIC.

- 
- [1] K. Langanke and G. Martínez-Pinedo, *Rev. Mod. Phys.* **75**, 819 (2003).
- [2] F. Osterfeld, *Rev. Mod. Phys.* **64**, 491 (1992), and references therein.
- [3] J. Rapaport and E. Sugarbaker, *Annu. Rev. Nucl. Part. Sci.* **44**, 109 (1994).
- [4] D. Frekers, *Prog. Part. Nucl. Phys.* **57**, 217 (2006).
- [5] Y. Fujita, B. Rubio, and W. Gelletly, *Prog. Part. Nucl. Phys.* **66**, 549 (2011).
- [6] A.L. Cole, H. Akimune, Sam M. Austin, D. Bazin, A.M. van den Berg, G.P.A. Berg, J. Brown, I. Daito, Y. Fujita, M. Fujiwara, S. Gupta, K. Hara, M.N. Harakeh, J. Jänecke, T. Kawabata, T. Nakamura, D.A. Roberts, B. M. Sherrill, M. Steiner, H. Ueno, and R. G. T. Zegers, *Phys. Rev. C* **74**, 034333 (2006).
- [7] T.N. Taddeucci, C.A. Goulding, T.A. Carey, R.C. Byrd, C.D. Goodman, C. Gaarde, J. Larsen, D. Horen, J. Rapaport, and E. Sugarbaker, *Nucl. Phys.* **A469**, 125 (1987), and references therein.
- [8] W.G. Love, K. Nakayama, and M.A. Franey, *Phys. Rev. Lett.* **59**, 1401 (1987).
- [9] M. Sasano, G. Perdikakis, R.G.T. Zegers, Sam M. Austin, D. Bazin, B.A. Brown, C. Caesar, A.L. Cole, J.M. Deaven, N. Ferrante, C.J. Guess, G.W. Hitt, R. Meharchand, F. Montes, J. Palardy, A. Prinke, L.A. Riley, H. Sakai, M. Scott, A. Stolz, L. Valdez, and K. Yako, *Phys. Rev. Lett.* **107**, 202501 (2011).
- [10] Y. Fujita, K. Hatanaka, G.P.A. Berg, K. Hosono, N. Matsuoka, S. Morinobu, T. Noro, M. Sato, K. Tamura, and H. Ueno, *Nucl. Instrum. Meth. Phys. Res. B* **126**, 274 (1997), and references therein.
- [11] H. Fujita, Y. Fujita, T. Adachi, A.D. Bacher, G.P.A. Berg, T. Black, E. Caurier, C.C. Foster, H. Fujimura, K. Hara, K. Harada, K. Hatanaka, J. Jänecke, J. Kamiya, Y. Kanzaki, K. Katori, T. Kawabata, K. Langanke, G. Martínez-Pinedo, T. Noro, D.A. Roberts, H. Sakaguchi, Y. Shimbara, T. Shinada, E.J. Stephenson, H. Ueno, T. Yamanaka, M. Yoshifuku, and M. Yosoi, *Phys. Rev. C* **75**, 034310 (2007).
- [12] Y. Fujita, Y. Shimbara, I. Hamamoto, T. Adachi, G.P.A. Berg, H. Fujimura, H. Fujita, J. Görres, K. Hara, K. Hatanaka, J. Kamiya, T. Kawabata, Y. Kitamura, Y. Shimizu, M. Uchida, H.P. Yoshida, M. Yoshifuku, and M. Yosoi, *Phys. Rev. C* **66**, 044313 (2002).
- [13] Y. Fujita, Y. Shimbara, A.F. Lisetskiy, T. Adachi, G.P.A. Berg, P. von Brentano, H. Fujimura, H. Fujita, K. Hatanaka, J. Kamiya, T. Kawabata, H. Nakada, K. Nakanishi, Y. Shimizu, M. Uchida, and M. Yosoi, *Phys. Rev. C* **67**, 064312 (2003).
- [14] Y. Fujita, H. Akimune, I. Daito, H. Fujimura, M. Fujiwara, M.N. Harakeh, T. Inomata, J. Jänecke, K. Katori, A. Tamii, M. Tanaka, H. Ueno, and M. Yosoi, *Phys. Rev. C* **59**, 90 (1999).
- [15] Y. Fujita, R. Neveling, H. Fujita, T. Adachi, N. T. Botha, K. Hatanaka, T. Kaneda, H. Matsubara, K. Nakanishi, Y. Sakemi, Y. Shimizu, F. D. Smit, A. Tamii, and M. Yosoi, *Phys. Rev. C* **75**, 057305 (2007).
- [16] T. Adachi, Y. Fujita, P. von Brentano, A.F. Lisetskiy, G.P.A. Berg, C. Fransen, D. De Frenne, H. Fujita, K. Fujita, K. Hatanaka, M. Honma, E. Jacobs, J. Kamiya, K. Kawase, T. Mizusaki, K. Nakanishi, A. Negret, T. Otsuka, N. Pietralla, L. Popescu, Y. Sakemi, Y. Shimbara, Y. Shimizu, Y. Tameshige, A. Tamii, M. Uchida, T. Wakasa, M. Yosoi, and K.O. Zell, *Phys. Rev. C* **73**, 024311 (2006).
- [17] Y. Fujita, T. Adachi, P. von Brentano, G.P.A. Berg, C. Fransen, D. De Frenne, H. Fujita, K. Fujita, K. Hatanaka, E. Jacobs, K. Nakanishi, A. Negret, N. Pietralla, L. Popescu, B. Rubio, Y. Sakemi, Y. Shimbara, Y. Shimizu, Y. Tameshige, A. Tamii, M. Yosoi, and K.O. Zell, *Phys. Rev. Lett.* **95**, 212501 (2005).
- [18] T. Adachi, Y. Fujita, A.D. Bacher, G.P.A. Berg, T. Black, D. De Frenne, C. C. Foster, H. Fujita, K. Fujita, K. Hatanaka, M. Honma, E. Jacobs, J. Jänecke, K. Kanzaki, K. Katori, K. Nakanishi, A. Negret, T. Otsuka, L. Popescu, D.A. Roberts, Y. Sakemi, Y. Shimbara, Y. Shimizu, E.J. Stephenson, Y. Tameshige, A. Tamii, M. Uchida, H. Ueno, T. Yamanaka, M. Yosoi, and K.O. Zell, *Phys. Rev. C* **85**, 024308 (2012).
- [19] L. Popescu, T. Adachi, G.P.A. Berg, P. von Brentano, D. Frekers, D. De Frenne, K. Fujita, Y. Fujita, E.-W. Grewe, M.N. Harakeh, K. Hatanaka, E. Jacobs, K. Nakanishi, A. Negret, Y. Sakemi, Y. Shimbara, Y. Shimizu, Y. Tameshige, A. Tamii, M. Uchida, H.J. Wortche, and M. Yosoi, *Phys. Rev. C* **79**, 064312 (2009).
- [20] <http://www.rcnp.osaka-u.ac.jp>.
- [21] T. Wakasa, K. Hatanaka, Y. Fujita, G.P.A. Berg, H. Fujimura, H. Fujita, M. Itoh, J. Kamiya, T. Kawabata, K. Nagayama, T. Noro, H. Sakaguchi, Y. Shimbara, H. Takeda, K. Tamura, H. Ueno, M. Uchida, M. Uraki, and M. Yosoi, *Nucl. Instrum. Meth. Phys. Res. A* **482**, 79 (2002).
- [22] M. Fujiwara, H. Akimune, I. Daito, H. Fujimura, Y. Fujita, K. Hatanaka, H. Ikegami, I. Katayama, K. Nagayama, N. Matsuoka, S. Morinobu, T. Noro, M. Yoshimura, H. Sakaguchi, Y. Sakemi, A. Tamii, and M. Yosoi, *Nucl. Instrum. Meth. Phys. Res. A* **422**, 484 (1999).
- [23] T. Noro *et al.*, RCNP (Osaka Univ.), Annual Report, 1991, p. 177.
- [24] H. Fujita, Y. Fujita, G.P.A. Berg, A.D. Bacher, C.C. Foster, K. Hara, K. Hatanaka, T. Kawabata, T. Noro, H. Sakaguchi, Y. Shimbara, T. Shinada, E.J. Stephenson, H. Ueno, and M. Yosoi, *Nucl. Instrum. Meth. Phys. Res. A* **484**, 17 (2002).



- [25] Y. Fujita, H. Fujita, G.P.A. Berg, K. Harada, K. Hatanaka, T. Kawabata, T. Noro, H. Sakaguchi, T. Shinada, Y. Shimbara, T. Taki, H. Ueno, and M. Yosoi, *J. Mass Spectrom. Soc. Jpn.* **48**(5), 306 (2000).
- [26] H. Fujita, G.P.A. Berg, Y. Fujita, K. Hatanaka, T. Noro, E.J. Stephenson, C.C. Foster, H. Sakaguchi, M. Itoh, T. Taki, K. Tamura, and H. Ueno, *Nucl. Instrum. Meth. Phys. Res. A* **469**, 55 (2001).
- [27] H. Fujita, *et al.*, RCNP (Osaka Univ.), Annual Report, 2010, p. 3.
- [28] T.W. Burrows, *Nuclear Data Sheets*, **108**, 923 (2007).
- [29] K. Matsuyanagi, *Prog. Theor. Phys.* **46**, 996 (1971).
- [30] A. Kuriyama, T. Marumori, and K. Matsuyanagi, *Prog. Theor. Phys.* **47**, 498 (1972).
- [31] DW81, a DWBA computer code by J. R. Comfort (1981) used in an updated version (1986), an extended version of DWBA70 by R. Schaeffer and J. Raynal (1970).
- [32] S.Y. van der Werf, S. Brandenburg, P. Grasdijk, W.A. Sterrenburg, M.N. Harakeh, M.B. Greenfield, B.A. Brown, and M. Fujiwara, *Nucl. Phys.* **A496**, 305 (1989).
- [33] R. Schaeffer, *Nucl. Phys.* **A164**, 145 (1971).
- [34] R.G.T. Zegers, H. Abend, H. Akimune, A.M. van den Berg, H. Fujimura, H. Fujita, Y. Fujita, M. Fujiwara, S. Galés, K. Hara, M.N. Harakeh, T. Ishikawa, T. Kawabata, K. Kawase, T. Mibe, K. Nakanishi, S. Nakayama, H. Toyokawa, M. Uchida, T. Yamagata, K. Yamasaki, and M. Yosoi, *Phys. Rev. Lett.* **90**, 202501 (2003).
- [35] T. Yamagata, H. Utsunomiya, M. Tanaka, S. Nakayama, N. Koori, A. Tamii, Y. Fujita, K. Katori, M. Inoue, M. Fujiwara, and H. Ogata, *Nucl. Phys.* **A589**, 425 (1995).
- [36] Y. Fujita, *Journal of Physics, Conference Series* **20**, 107 (2005).
- [37] T. Adachi, Y. Fujita, P. von Brentano, G.P.A. Berg, C. Fransen, D. De Frenne, H. Fujita, K. Fujita, K. Hatanaka, M. Honma, E. Jacobs, J. Kamiya, K. Kawase, T. Mizusaki, K. Nakanishi, A. Negret, T. Otsuka, N. Pietralla, L. Popescu, Y. Sakemi, Y. Shimbara, Y. Shimizu, Y. Tameshige, A. Tamii, M. Uchida, T. Wakasa, M. Yosoi, and K.O. Zell, *Nucl. Phys.* **A788**, 70c (2007).
- [38] Y. Fujita *et al.*, RCNP (Osaka Univ.), Annual Report, 2010, p. 1.
- [39] Y. Fujita *et al.*, RCNP (Osaka Univ.), Annual Report, 2010, p. 2.
- [40] J. Jänecke, K. Pham, D.A. Roberts, D. Stewart, M.N. Harakeh, G.P.A. Berg, C.C. Foster, J.E. Lisantti, R. Sawafu, E.J. Stephenson, A.M. van den Berg, S.Y. van der Werf, S.E. Muraviev, and M.H. Urin, *Phys. Rev. C* **48**, 2828 (1993).
- [41] Y. Shimbara, Y. Fujita, T. Adachi, G.P.A. Berg, H. Fujimura, H. Fujita, K. Fujita, K. Hara, K.Y. Hara, K. Hatanaka, J. Kamiya, K. Katori, T. Kawabata, K. Nakanishi, G. Martinez-Pinedo, N. Sakamoto, Y. Sakemi, Y. Shimizu, Y. Tameshige, M. Uchida, M. Yoshifuku, and M. Yosoi, *Phys. Rev. C* **86**, 024312 (2012).
- [42] M. Honma, T. Otsuka, B.A. Brown, and T. Mizusaki, *Phys. Rev. C* **69**, 034335 (2004).
- [43] G. Martinez-Pinedo, A. Poves, E. Caurier, and A.P. Zuker, *Phys. Rev. C* **53**, R2602 (1996).
- [44] A. Poves, J. Sánchez-Solano, E. Caurier, and F. Nowacki, *Nucl. Phys.* **A694**, 157 (2001).
- [45] <http://www.nscl.msu.edu/brown/resources/resources.html>.
- [46] Y. Fujita, B.A. Brown, H. Ejiri, K. Katori, S. Mizutori, and H. Ueno, *Phys. Rev. C* **62**, 044314 (2000), and references therein.
- [47] E.K. Warburton and J. Weneser, in *Isospin in Nuclear Physics*, edited by D.H. Wilkinson (North-Holland, Amsterdam, 1969), Chap. 5, and references therein.
- [48] S.S. Hanna, in *Isospin in Nuclear Physics*, edited by D.H. Wilkinson (North-Holland, Amsterdam, 1969), Chap. 12, and references therein.
- [49] H. Morinaga and T. Yamazaki, *In-Beam Gamma-Ray Spectroscopy* (North-Holland, Amsterdam, 1976), and references therein.
- [50] Y. Shimbara, Y. Fujita, T. Adachi, G.P.A. Berg, H. Fujita, K. Fujita, I. Hamamoto, K. Hatanaka, J. Kamiya, K. Nakanishi, Y. Sakemi, Y. Shimizu, M. Uchida, T. Wakasa, and M. Yosoi, *Eur. Phys. J. A* **19**, 25 (2004).
- [51] Y. Fujita, I. Hamamoto, H. Fujita, Y. Shimbara, T. Adachi, G.P.A. Berg, K. Fujita, K. Hatanaka, J. Kamiya, K. Nakanishi, Y. Sakemi, Y. Shimizu, M. Uchida, T. Wakasa, and M. Yosoi, *Phys. Rev. Lett.* **92**, 062502 (2004).
- [52] P. Moller, and J.R. Nix, W.D. Myers, W.J. Swiatecki, *Atomic Data Nucl. Data Tables* **59**, 185 (1995).
- [53] Y. Fujita, Y. Shimbara, T. Adachi, G.P.A. Berg, B.A. Brown, H. Fujita, K. Hatanaka, J. Kamiya, K. Nakanishi, Y. Sakemi, S. Sasaki, Y. Shimizu, Y. Tameshige, M. Uchida, T. Wakasa, and M. Yosoi, *Phys. Rev. C* **70**, 054311 (2004).
- [54] J.P. Schiffer and W.W. True, *Rev. Mod. Phys.* **48**, 191 (1996).
- [55] C. Dossat, N. Adimi, F. Aksouh, F. Becker, A. Bey, B. Blank, C. Borcea, R. Borcea, A. Boston, M. Caa-mano, G. Cachel, M. Chartier, D. Cortina, S. Czajkowski, G. de France, F. de Oliveira Santos, A. Fleury, G. Georgiev, J. Giovinnazzo, S. Grévy, R. Grzywacz, M. Hellström, M. Honma, Z. Janas, D. Karamanis, J. Kurcewicz, M. Lewitowicz, M.J. López Jiménez, C. Mazzocchi, I. Matea, V. Maslov, P. Mayet, C. Moore, M. Pfützner, M.S. Pravikoff, M. Stanoiu, I. Stefan, and J.C. Thomas, *Nucl. Phys.* **A792**, 18 (2007).
- [56] A. Bohr and B. Mottelson, *Nuclear Structure* (Benjamin, New York, 1975), Vol. 2, Chap. 6.